Research Article

Transcriptional and post-transcriptional regulation of oxytocin and vasopressin gene expression by CREB3L1 and CAPRIN2

Soledad Bárez-López[a], Agnieszka Konopacka[a†], Stephen J Cross[b], Mingkwan Greenwood[a], Marina Skarveli[a], David Murphy[a*] and Michael P. Greenwood[a*]

[a] Molecular Neuroendocrinology Research Group, Bristol Medical School: Translational Health Sciences, University of Bristol, Dorothy Hodgkin Building, Bristol, United Kingdom.
[b] Wolfson Bioimaging Facility, Biomedical Sciences Building, University of Bristol, Bristol, United Kingdom.
[†]Present address: GlaxoSmithKline, Protein Degradation Group, Medicines Research Centre, Gunnels Wood Road, Stevenage, UK.
[*]Equal senior authors

Short Title: regulation of *Avp* and *Oxt* by CREB3L1 and CAPRIN2

Corresponding Author:

Michael Paul Greenwood

Molecular Neuroendocrinology Research Group, Bristol Medical School: Translational Health Sciences, University of Bristol.

Dorothy Hodgkin Building, Whitson Street, Bristol

Whitson Street, Bristol

Tel: +44 117 331 3071

E-mail: mike.greenwood@bristol.ac.uk

Number of Tables: 0.

Number of Figures: 9.

Word count: 5968.

Keywords: vasopressin, oxytocin, CAPRIN2, CREB3L1.

Abstract

Introduction: Water homeostasis is achieved by secretion of the peptide hormones arginine vasopressin (AVP) and oxytocin (OXT) that are synthesised by separate populations of magnocellular neurones (MCNs) in the supraoptic (SON) and paraventricular (PVN) nuclei of the hypothalamus. To further understand the molecular mechanisms that facilitate biosynthesis of AVP and OXT by MCNs, we have explored the spatiotemporal dynamic, both mRNA and protein expression, of two genes identified by our group as being important components of the osmotic defence response: *Caprin2* and *Creb3l1*.

Methods: By RNA *in situ* hybridization and immunohistochemistry, we have characterised the expression of *Caprin2* and *Creb3l1* in MCNs in the basal state, in response to dehydration, and during rehydration in the rat.

Results: We found that *Caprin2* and *Creb3l1* are expressed in AVP and OXT MCNs and in response to dehydration expression increases in both MCN populations. Protein levels mirror the increase in transcript levels for both CREB3L1 and CAPRIN2. In view of increased CREB3L1 and CAPRIN2 expression in OXT neurones by dehydration, we explored OXT specific functions for these genes. By luciferase assays, we demonstrate that CREB3L1 may be a transcription factor regulating *Oxt* gene expression. By RNA immunoprecipitation assays and northern blot analysis of *Oxt* mRNA poly(A) tails, we have found that CAPRIN2 binds to *Oxt* mRNA and regulates its poly(A) tail length. Moreover, in response to dehydration, *Caprin2* mRNA is subjected to nuclear retention, possibly to regulate *Caprin2* mRNA availability in the cytoplasm.

Conclusion: The exploration of the spatiotemporal dynamics of *Creb3l1* and *Caprin2* encoded mRNAs and proteins has provided novel insights beyond the AVP-ergic system revealing novel OXT-ergic system roles of these genes in the osmotic defence response.

Introduction

Optimal bodily water content is essential for survival, good health and wellbeing, and when threatened, osmotic stability is aggressively defended. The brain mechanisms regulating water balance are mediated by magnocellular neurones (MCNs) of the supraoptic nucleus (SON) and paraventricular nucleus (PVN) of the hypothalamus. MCNs synthesise the peptide hormones arginine vasopressin (AVP) and oxytocin (OXT) in their cell bodies and project their axons to blood capillaries of the posterior pituitary (PP) gland. AVP and OXT are transported down these axons and stored in terminals at the neuro-vascular interface of the PP. In response to stimulation, AVP and OXT are secreted into the systemic circulation, acting as hormones on remote targets [1]. Regarding water balance, upon hyperosmotic stress, for example chronic dehydration, AVP is released into the bloodstream to act at the kidney collecting duct to promote water reabsorption [2]. The role of OXT in osmotic regulation is related to natriuresis as in response to hyperosmotic stimulation (including salt loading [3], hypertonic NaCl infusion [4] and chronic dehydration [5]) OXT is released to increase sodium excretion to facilitate sodium homeostasis [3, 6, 7]. Chronic osmotic stimulation leads to the depletion of AVP and OXT pituitary stores and, consequently, demands increased synthesis of AVP and OXT in MCNs to ensure adequate supply. This starts with an increase in gene transcription, which results in an increase in the abundance of the precursor *Avp* [8] and *Oxt* [9] heteronuclear RNAs, and the mature *Avp* [10] and *Oxt* [11, 12] mRNAs. Moreover, hyperosmotic stimulation also increases the poly(A) tail lengths of *Avp* and *Oxt* mRNA, possibly to enhance transcript stability and/or translation [13-15].

Due to the importance of water homeostasis for health and wellbeing, it is essential to understand cellular mechanisms that mediate AVP and OXT synthesis. We previously identified cAMP responsive element binding protein 3 like 1 (CREB3L1) as a transcription factor that regulates *Avp* gene expression [16]. CREB3L1 is a transcription factor of the CREB/activating transcription factor family, and its expression increases in parallel with *Avp* gene expression in response to hyperosmotic stimuli in both the SON and PVN [17, 16]. CREB3L1 positively regulates the expression of *Avp* in response to increases in cAMP levels by directly binding to the *Avp* promoter [16, 18]. Though CREB3L1 is expressed in OXT neurones its function is not known.

We have also identified a novel post-transcriptional mechanism controlling the AVP mRNA poly(A) tail length involving RNA binding protein *Caprin2* [19], a central hub gene of a network of genes involved in the osmotic stress defence response [20], which increases in expression in the SON and PVN in response to hyperosmotic stimuli [21]. We have shown that CAPRIN2 binds to the *Avp* mRNA and mediates an increase in the length of the poly(A) tail and *Avp* mRNA abundance [21]. Whilst much is known regarding the mechanisms regulating *Avp* gene transcription and mRNA poly(A) tail length, our understanding of mechanisms controlling *Oxt* gene expression and changes to its mRNA poly(A) tail length currently lag behind.

In order to gain further insight into the roles of CREB3L1 and CAPRIN2 in the osmotic stress defence response, we have explored the spatiotemporal dynamics of *Creb3l1* and *Caprin2* mRNA and CREB3L1 and CAPRIN2 protein during dehydration and following recovery by rehydration. We used RNAscope *in situ* hybridization and immunohistological approaches to determine the expression at mRNA and protein levels in the SON and the PVN. We found that *Creb3l1* is mainly expressed in AVP, but also present in OXT MCNs. Moreover, in response to dehydration, *Creb3l1* mRNA and CREB3L1 protein abundance increased in both AVP and OXT neurones, although to a greater extent in the former. We also show that *Caprin2* is expressed in both AVP and OXT neurones and that, in response

to dehydration, *Caprin2* mRNA and CAPRIN2 protein levels increase in both cell types to the same extent. We further explored the role of these genes in the OXT-ergic system. We found that CREB3L1 can regulate *Oxt* transcription by luciferase assays and that CAPRIN2 binds *Oxt* mRNA and regulates its poly(A) tail length. In addition, we found prominent nuclear *Caprin2* mRNA aggregates in response to osmotic stimulation, possibly to regulate *Caprin2* mRNA availability to the cytoplasm in response to dehydration. Together, these data endorse our approach to exploring the spatiotemporal dynamics of genes in the SON, providing novel insights about the roles of CREB3L1 and CAPRIN2 in the OXT-ergic system in response to dehydration.

Materials and Methods

Animals

Male Sprague-Dawley rats (purchased from Envigo) weighing 250–300 g were used in this study. Rats were maintained under a 14:10 light dark cycle (lights on 5.00 am) at a constant temperature of 22°C and a relative humidity of 50%-60% and housed in groups with environmental enrichment consisting of nesting material, cardboard tube, and a chew block. Rats were acclimatised for 1 week prior to experimentation, where they had *ad libitum* access to food and water. Animal experiments were terminated between 9.00 am and 2.00 pm. Rats were euthanised by striking of the cranium. Brains were removed and immediately frozen in powdered dry ice and stored at −80°C.

Osmotic stimulation protocols

For *in situ* hybridization and immunohistochemistry studies, we used a dehydration protocol where water, but not food, was removed for 72 hours. In a rehydration protocol, water was reintroduced following 72 hours dehydration for 4, 8 and 24 hours prior to sample collection. Rats were randomly allocated into one of five groups: euhydrated or control, with *ad libitum* access to food and water; 72 hours dehydration; 72 hours dehydration followed by 4 hours rehydration; 72 hours dehydration followed by 8 hours rehydration and 72 hours dehydration followed by 24 hours rehydration.

For RNA immunoprecipitation assays, we used a chronic hypertonic protocol where drinking water was replaced with 2% (wt/vol) NaCl for 7 days (salt-loaded). Control euhydrated rats were compared to salt-loaded animals.

RNAscope in situ hybridization

Frozen brains were sliced into 16 µm coronal sections and mounted on Superfrost Plus slides (Thermo Fisher Scientific, Waltham, MA, USA) and stored -80 until used. The fresh frozen brain sections were fixed in ice-cold 4% paraformaldehyde for 15 min, washed in PBS and dehydrated in ascending (50%, 70%, and 2 · 100%) ethanol concentrations for 5 min each. The tissue was treated with RNAscope IV protease reagent (Advanced Cell Diagnostics, 320850) for 30 min at RT and washed twice in water. RNAscope probes were hybridized for 2 hours at 40° in a HybEZ oven (Advanced Cell Diagnostics, Newark, CA, USA). The probes Rn-AVP-C2 (Advanced Cell Diagnostics , 401421-C2) targeting 20 – 525 of rat *Avp* gene, Rn-Caprin2-C3 (Advanced Cell Diagnostics, 578421-C3) targeting 915-1898 of rat *Caprin2* gene (spanning at least 5 exons, and therefore labelling mature *Caprin2* mRNA), Rn-Creb3l1-C3 (Advanced Cell Diagnostics, 485691-C3) targeting 1316 – 2287 of rat *Creb3l1* gene (spanning 7 exons, and therefore labelling mature *Creb3l1* mRNA), Rn-Malat1 (Advanced Cell Diagnostics, 404421) targeting 469 – 1429 of rat *Malat1* gene and Rn-Oxt (Advanced Cell Diagnostics, 479631) targeting 2–490 of rat *Oxt* gene were designed and manufactured by Advanced Cell Diagnostics. The probes were incubated in these combinations: 1) Rn-Oxt, Rn-AVP-C2 and Rn-

Caprin2-C3, 2) Rn-Oxt, Rn-AVP-C2 and Rn-Creb3l1-C3 and 3) Rn-Malat1 and Rn-Caprin2-C3. Signal amplification was performed using the RNAscope Multiplex Fluorescent Reagent Kit (Advanced Cell Diagnostics, 320850) following the manufacturer's guidelines and using amplifier 4A.

Combined RNAscope in situ hybridization and immunohistochemistry

For combined RNA Scope *in situ* hybridization for *Caprin2* and *Creb3l1* with immunohistochemistry for CAPRIN2 and CREB3L1, the RNA scope *in situ* hybridization protocol was performed as described above, with the exception that the tissue was treated with RNAscope III protease reagent (Advanced Cell Diagnostics, 233337), instead of RNAscope IV protease reagent, for 20 min at RT. Following signal amplification with the RNAscope Multiplex Fluorescent Reagent Kit, the sections were blocked in PBS containing 0.1% Triton X-100, 4% bovine serum albumin (BSA), and 5% donkey serum at RT for 1 hour to prevent nonspecific protein binding. Next, tissue sections were incubated at 4°C either with a primary antibody against CAPRIN2 (1:150; Proteintech, 20766-1-AP) overnight or CREB3L1 (1:200; R&D Systems, AF4080) for 72 hours in PBS containing 0.1% Triton X-100, 4% BSA, and 1% donkey serum. The secondary antibodies donkey anti-rabbit Alexa Fluor Plus 488 (Invitrogen, A32790) and donkey anti-goat Alexa Fluor 488 (Invitrogen, A11055) were used to label CAPRIN2 and CREB3L1, respectively, at a 1:500 dilution in PBS containing 0.1% Triton, 4% BSA, and 1% donkey serum at RT for 1 h. The slices were then washed in PBS and incubated with 4',6-Diamidino-2-phenylindole dihydrochloride (DAPI, D1306; Molecular Probes) in PBS. After washing in PBS, slices were mounted with ProLong Gold Antifade Mountant (Invitrogen, P36930).

For combined RNAscope *in situ* hybridization for *Caprin2* with immunohistochemistry against nuclear markers, the RNA scope *in situ* hybridization protocol was performed as described in the "RNAscope in situ hybridization Protocol" section, but in this case no tissue dehydration or protease treatment was performed. So, after fixation in 4% paraformaldehyde for 15 min and PBS washes, the sections were immediately incubated with the Rn-Caprin2-C3 probe. Following signal amplification with the RNAscope Multiplex Fluorescent Reagent Kit, the immunohistochemistry was performed as described above. Subnuclear regions were labelled with antibodies against COILIN (1:200; MyBioSource, MBS9603377), FIBRILLARIN (1:50, Santa Cruz, sc-374022), PSPC1 (1:250; Novus Biologicals, NBP1-83801) and SC35 (1:100; Novus Biologicals, NB100-1774).

Image acquisition and data analysis

Image acquisition was performed with a Leica SP5-II AOBS confocal laser scanning microscope attached to a Leica DMI 6000 inverted epifluorescence microscope. Images for *Oxt-Avp-Caprin2* and *Oxt-Avp-Creb3l1* RNAscope experiments as well as for combined RNAscope and immunohistochemistry for Caprin2 and Creb3l1 mRNA and proteins, images were captured using a 20x and a 63x PL APO CS lens with a 3.4-zoom factor. For combinations of RNAscope with nuclear markers, immunohistochemistry and *Malat1-Caprin2* RNAscope, images were captured with a 63x PL APO CS lens and a 6-zoom factor and Z stacks (Z step size = 0.17 µm) were taken for all images. Raw image files were processed to generate composite images using the open access image analysis software, Fiji.

Quantification of RNA dots in the nucleus (DAPI labelling close to either AVP- or OXT-positive cytoplasm) or cytoplasm (AVP or OXT labelling) of AVP or OXT neurones was performed using the Modular Image Analysis (MIA), modular workflow plugin for Fiji. In this workflow, nuclei were detected using an Otsu threshold- and watershed-based approach, with individual nuclei identified as contiguous regions of foreground-labelled pixels larger than a specified area. Likewise, cytoplasmic regions were identified as contiguous foreground-labelled regions following manual intensity

thresholding. Any cytoplasmic regions overlapping previously-detected nuclei were discarded to ensure mutual spatial exclusivity. RNA dots were identified using the TrackMate plugin for Fiji and related to the nuclear or cytoplasmic region with which they overlapped. Quantification was performed on the entire image acquired with 63x PL APO CS lens and a 3.4 zoom factor. Results are presented as the ratio of the number of RNA dots representing (Caprin2 or Creb3l1 RNA molecules)/µm² area (OXT nucleus, OXT cytoplasm, AVP nucleus or AVP cytoplasm).

Luciferase assays

Luciferase assays were performed as described [16]. In short, plasmid constructs expressing the full-length rat CREB3L1 (CREB3L1FL) were cloned into the pcDNA3 plasmid and plasmid constructs expressing the constitutively active form of mouse CREB3L1 (CREB3L1CA) cloned into pcDNA3 was kindly provided by Kazunori Imaizumi (University of Miyazaki, Miyazaki, Japan). A region of the rat oxytocin promoter (-3187 - -1 bp) was amplified from genomic DNA (5'-CACCCCTTCATGCCTGCAA-3' and 5'-CCGCTCGAGTGGTTTCTCCAGCCCAGACCGACCTT-3') and cloned into pGEM-T easy vector (Promega). Deletion mutants were generated by restriction digestion (*KpnI* for -822 to -1 bp and *SacI* for -197 to -1 bp) and cloned into corresponding sites of pGL3 luciferase plasmid (Promega). Luciferase assays were performed in HEK293T cells following the Promega Dual-Luciferase Reporter Assay System protocol with pRL-TK (Promega) control reporter vector. Luciferase activity was measured on a Lumat LB 9507 Luminometer (Berthold Technologies) in triplicate.

Introduction of viral vectors into the hypothalamus

CAPRIN2 was knocked down in the SON and the PVN as described [21]. Briefly, Caprin2 short hairpin RNA (shRNA) or scrambled shRNA were cloned into lentivirus pRRL.sin.U6.shRNA.cppt.CMV.GFP [21]. These constructs were delivered bilaterally into the SON and the PVN. Rats were anaesthetised by intramuscular administration of ketamine (100 mg/kg) and medetomidine hydrochloride (0.3 mg/kg) and placed in a stereotaxic frame. An incision was made at the midline to expose the skull and 4 holes were drilled through the skull: 2 for SON (1.3 mm posterior to bregma and ± 1.95 mm lateral to bregma) and 2 for PVN (1.8 mm posterior to bregma and ± 0.4 mm lateral to bregma). 1 µl of lentivirus expressing Caprin2 shRNA or scrambled shRNA at the concentration of 2×10^9 TU/ml was administered above the nucleus over 5 minutes using fine pulled glass pipettes as described [21]. Four weeks following surgery, rats were salt-loaded for 7 days before sample collection. Accuracy of viral delivery and knockdown was confirmed by *egfp* and *Caprin2* mRNA expression analysis in each injected nuclei by qRT-PCR. The total RNA from salt-loaded scrambled shRNA-injected rats (n = 5) and salt-loaded Caprin2 shRNA-injected rats (n=5) was used for Northern blot analysis.

RNA immunoprecipitation assay

SON and PVN samples were obtained by punching out the nuclei using a 1 mm tissue punch tool from 60 µm frozen sections sliced in a cryostat [21]. The accuracy of punch collection was monitored by staining punched slices with 2% (wt/vol) toluidine blue. Immunoprecipitation was performed as described [21]. Briefly, tissue punches from both SON or PVN were cross-linked with 1% (vol/vol) formaldehyde in PBS for 10 min at RT followed by a 5 min incubation with 0.125 M glycine (pH 7.0). Samples were washed 3 times in PBS by centrifuging for 5 min at 2000×g, 4°C. Then, the samples were homogenised in 100 µl of NT- RNA immunoprecipitation buffer containing 50 mM Tris, pH 7.4, 150 mM NaCl, 1 mM MgCl2, 0.5% Nonidet P40, 1 mM EDTA pH 8.0, 1 mM DTT, complete protease inhibitor (Roche), and 200 U/ml RNase Out (Invitrogen, USA), incubated for 10 min at 4°C and pre-cleared with 25 µl of Protein G-coated Dynabeads (Life Technologies). Protein levels were determined by BCA protein assay. SON and PVN samples containing 30 µg and 60 µg of protein,

respectively, were incubated overnight at 4°C with either goat anti-Caprin-2 antibody (Santa Cruz Biotechnology, sc-107473) or with non-specific goat IgG (Santa Cruz Biotechnology, sc-2028) at a concentration ratio 1:8, in PBS containing RNase Out (200 U/ml) and Complete Protease Inhibitor. The following day, the protein-antibody extracts were incubated with G-protein Dynabeads for 2 hr at 4°C. The protein-G-adsorbed complexes were washed with PBS and washed out with 50 µl of crosslinking reversal buffer (50 mM Tris-HCl pH 7.0, 5 mM EDTA, 10 mM DTT, 200 U/ml RNase Out) for 45 min at 70°. Total RNA was isolated and used for qRT-PCR analysis as described [21] using the OXT primers F 5'CTTGGCCTACTGGCTCTGAC, R 5'GTCCGCAGGGAAGACACT and the Gapdh primers F 5'ATGATTCTACCCACGGCAAG, R 5'CTGGAAGATGGTGATGGGTT.

Northern blot analysis of mRNA poly(A) tails

Northern blot analysis was performed using total RNA extracted from SONs and PVNs of rats injected with lentiviruses delivering Caprin2 shRNA or scrambled shRNA, using Ambion NorthernMax kit (Life Technologies) as described [21]. The sequences of the anti-sense (AS) oligonucleotide probes used were:

rOXT-AS–5' TGGCCATGGGGAATGAAGGAAGCGCCCTAAAGGTATCATCACAAAGC 3'

rGAPDH-AS–5' CCAGCCTTCTCCATGGTGGTGAAGACGCCAGTAGACTCCACGACA 3'.

Statistical analysis

Data are presented as mean ± SD. Statistical analyses were performed with GraphPad Prism software v8 (GraphPad). Assessment of the normality of data was performed by Shapiro-Wilk test. Means between two groups were compared by 2-tailed, unpaired Student's t-test for parametric and differences between means for more than two groups was performed by one-way analysis of variance (ANOVA) and the Bonferroni's post hoc test to correct for multiple comparisons for parametric data and by Kruskal-Wallis test for non-parametric data. Significant differences are presented as *P < 0.05; **P < 0.01, and ***P < 0.001.

Results

Anatomical patterns of Creb31l and Caprin2 gene expression

In order to fully characterise the anatomical patterns of *Creb3l1* and *Caprin2* expression, we performed RNAscope *in situ* hybridization labelling of *Creb3l1* or *Caprin2* in combination with *Avp* and *Oxt* to mark AVP and OXT MCNs, respectively. We investigated expression in the SON and PVN of euhydrated and dehydrated rats, and during 4, 8 or 24 hours of rehydration.

Analysis of *Creb3l1* transcript expression in the SON revealed that, in euhydrated conditions, *Creb3l1* RNA is expressed in AVP and OXT MCNs both in the nucleus and cytoplasm compartments (Fig. 1a, j, l). Dehydration increased *Creb3l1* RNA abundance in the cytoplasm and nucleus of both AVP (6.1- and 7.7-fold in the cytoplasm [Fig. 1b, f] and nucleus [Fig. 1b, g], respectively) and OXT neurones (9.6- and 4.6-fold in the cytoplasm [Fig. 1b, h] and nucleus [Fig. 1b, i], respectively). Notably, *Creb3l1* RNA expression is 3.5-fold higher in the cytoplasm (Fig. 1k) and nucleus (Fig. 1m) of AVP in comparison to OXT MCNs. During rehydration, *Creb3l1* expression gradually decreases in the cytoplasm and nucleus of AVP and OXT cells and by 24 hours is not significantly different from euhydrated controls (Fig. 1e, f, g, h, i). Analysis of *Creb3l1* expression in the PVN revealed that *Creb3l1* is preferentially expressed in AVP neurones being 4.8-fold higher in the cytoplasm of AVP compared to OXT neurones (Fig. 2 a, j). In response to dehydration, *Creb3l1* increases in AVP neurones (9- and 6.8-fold increase in the

cytoplasm [Fig. 2b, f] and nucleus [Fig. 2b, g], respectively) and by 24 hours is not statistically significant different from euhydrated levels in either compartment (Fig. 2 e, f, g, h, i). In OXT neurones *Creb3l1* expression increases 4.2-fold in the cytoplasm (Fig. 2b, h) and 2.3 in the nucleus (Fig. 2b, i) in response to dehydration, but this increase is not significantly different from control values. Of note, under osmotic stress conditions *Creb3l1* expression is 9.2- and 6.8-fold higher in the cytoplasm (Fig. 2k) and nucleus (Fig. 2m), respectively, of AVP in comparison to OXT neurones.

In the SON, *Caprin2* is expressed in AVP and OXT neurones in the euhydrated state (Fig. 3a, j, l). Dehydration robustly increases *Caprin2* expression in the nucleus and cytoplasm of both AVP (4.7- and 4-fold increase in the cytoplasm [Fig. 3b, f] and nucleus [Fig. 3b, g], respectively) and OXT (4.9- and 7-fold increase in the cytoplasm [Fig. 3b, h] and nucleus [Fig. 3b, i], respectively) neurones with no differences in the expression of *Caprin2* between AVP and OXT neurons (Fig. 3b, k, m). During rehydration, *Caprin2* expression decreases in the cytoplasm and nucleus of AVP and OXT neurones. After 24 hours there is no statistically significant difference from control euhydrated levels (Fig. 3 e, f, g, h, i). In the PVN, *Caprin2* is also equally expressed both in AVP and OXT neurons in the euhydrated basal state in cytoplasm (Fig. 4a, j) and nucleus (Fig. 4a, l) of AVP and OXT cells. Dehydration increases *Caprin2* expression in the nucleus and cytoplasm of both AVP (5- and 4.8-fold increase in the cytoplasm [Fig. 4b, f] and nucleus [Fig. 4b, g], respectively) and OXT (8.2- and 10.4-fold increase in the cytoplasm [Fig. 4b, h] and nucleus [Fig. 4b, i], respectively) neurones. However, in this case *Caprin2* only increases to the same extent in the cytoplasm of AVP and OXT neurones in response to dehydration (Fig. 4k), but the expression in the nucleus of OXT cells is 2.7-fold higher than in AVP neurones (Fig. 4m). Rehydration decreases cytoplasm and nuclear abundance of AVP and OXT neurones returning to basal levels by 24 hours (Fig. 4e, f, g, h, i).

Interestingly, *in situ* hybridization analysis revealed very prominent *Caprin2* mRNA aggregates in the nucleus. These *Caprin2* mRNA nuclear aggregates are present in basal euhydrated conditions (Figs. 3a, 4a) and greatly increase in number and size in response to dehydration, both in the SON and the PVN (Figs. 3b, 4b). This suggests that, especially during dehydration, there is nuclear retention of mature *Caprin2* mRNA.

Gene and protein expression dynamics of Creb3l1 and Caprin2

It is well accepted that mRNA and protein concentrations do not necessarily correlate [22, 23]. To assess whether the differential *Creb3l1* and *Caprin2* mRNA expression during dehydration reflects changes in protein levels, and hence has biological implications, we performed combined RNAscope *in situ* hybridization and immunohistochemistry for *Creb3l1* and *Caprin2* mRNA and CREB3L1 and CAPRIN2 protein. In euhydrated conditions *Creb3l1* expression was detected in MCNs of the SON or the PVN (Fig. 5a). In response to dehydration, *Creb3l1* RNA increased 6.6- and 4.6-fold in the cytoplasm (Fig. 5b, g) and nucleus (Fig. 5b, h), respectively, whilst CREB3L1 protein expression increased 2.5-fold throughout the cell cytoplasm of MCNs in the SON (Fig 5b, i). During rehydration both mRNA and protein levels returned to euhydrated basal levels in the SON (Fig. 5c, g, h, i). In the PVN, dehydration led to increases in *Creb3l1* RNA levels that were 9.8-fold higher in the cytoplasm (Fig. 5e, j) and 7.8-fold higher in the nucleus (Fig. 5e, k). Accordingly, CREB3L1 protein staining increased 1.8-fold in MCNs of the PVN (Fig. 5e, l) in response to dehydration but was not statistically significant. Since CREB3L1 protein staining measurements were not restricted to MCNs, the lack of significance could be due to increased variability in protein intensity from non-MCNs. During rehydration both mRNA and protein levels returned to basal levels in the PVN (Fig. 5f, j,k,l).

Staining for CAPRIN2 is detectable in euhydrated conditions in MCNs of the SON (Fig. 6a) and the PVN (Fig. 6d). In dehydration, *Caprin2* RNA increased 3.1-fold in the cytoplasm (Fig. 6b, g) and 2.9-fold in the nucleus (Fig. 6b, h), and CAPRIN2 protein staining also increased 2.9-fold in the MCNs of the SON (Fig. 6b, i). During rehydration, *Caprin2* mRNA and CAPRIN2 protein levels returned to euhydrated basal levels in the SON (Fig. 6c, g, h, i). In the PVN, *Caprin2* RNA increased 2.6-fold in the cytoplasm (Fig. 6e, j) and 2.8-fold in the nucleus (Fig. 6e, k) in response to dehydration. CAPRIN2 protein levels, increased 2.6-fold in MCNs of the PVN as a result of dehydration (Fig. 6e, l). During rehydration *Caprin2* mRNA and CAPRIN2 protein levels progressively returned to basal levels in the PVN (Fig. 6f, j, k, l).

Nuclear Caprin2 mRNA aggregates are not restricted to specific nuclear domains

To gain further insight into the sub-nuclear localisation of the *Caprin2* mRNA aggregates, we performed RNA *in situ* hybridization for *Caprin2* mRNA in combination with immunohistochemistry for several nuclear compartment proteins in the SON of dehydrated rats. One exception being *Caprin2* mRNA in combination with the *Malat1* RNA nuclear speckle marker by *in situ* hybridization. We did not observe overlap in the localisation of *Caprin2* mRNA and immunolabelling with an antibody against FIBRILLARIN, a marker for the nucleolus (Fig. 7a''), which is a site for ribosome biogenesis [24]. There was no co-localisation with Cajal body marker COILIN (Fig. 7b'') which are sites of transcriptional activation, mRNA processing and assembly of small ribonucleoproteins [25]. Neither did *Caprin2* mRNA localise with PSPC1 (Fig. 7c''), which is a marker for paraspeckles which are known to regulate gene expression by nuclear retention of double-stranded RNA structures, normally formed by inverted repeats [26]. In addition, *Caprin2* mRNA aggregates were not exclusively observed in nuclear speckles which are believed to have a role in recycling and coordinating the supply of splicing factors to sites of transcription [27, 28], with no overlap in the expression of SC35 (Fig. 7d'') or *Malat1* RNA (Fig. 7e''). These data suggest that *Caprin2* mRNA nuclear aggregates are not spatially correlated with any of the nuclear domains currently explored.

CREB3L1 can regulate Oxt transcription

The presence of CREB3L1 in OXT neurones and the fact *Creb3l1* increases in this cell type in response to osmotic stress, suggested that CREB3L1 may regulate *Oxt* gene expression. To investigate transcriptional regulation of the OXT gene by CREB3L1, we performed luciferase assays using a proximal *Oxt* promoter region transfected in HEK293T cells. The expression of full-length CREB3L1 (CREB3L1FL) and a constitutively active CREB3L1 (CREB3L1CA) significantly increased luciferase activity by 5.4- and 3.2-fold, respectively, compared with controls (Fig. 8a). Moreover, truncating the *Oxt* promoter from 822 bp to 197 bp did not diminish luciferase activity remaining 5.2- and 6.7-fold higher, respectively (Fig. 8b). This suggests that CREB3L1 actions on the *Oxt* promoter are probably mediated by sequences located in this 197 bp region upstream the of the transcription start site of the *Oxt* gene. Studies have shown that the proximal region of the *Oxt* promoter is targeted by a number of hormone receptors, for example the oestrogen receptor, as well as several orphan receptors [2]. Interestingly, no canonical CREB3L1 binding motifs were found to exist within this region (Fig. 8c).

CAPRIN2 binds to Oxt mRNA and regulates its poly(A) tail length

We have previously demonstrated that CAPRIN2 binds to *Avp* mRNA and enhances its mRNA poly(A) tail, thereby increasing transcript stability [21]. The present findings indicate that CAPRIN2 also mediates a relevant role in the OXT-ergic system in response to dehydration. In order to assess if CAPRIN2 can also bind the *Oxt* mRNA, we performed RNA immunoprecipitation assays on SON and

PVN extracts of euhydrated and osmotically stimulated rats by salt loading. To this aim, qPCR analysis of *Oxt* mRNA levels were performed following incubation of the hypothalamic extracts with antibodies recognising CAPRIN2 and a control IgG. We found that *Oxt* mRNA levels in the euhydrated SON and PVN were, respectively, 35.9- and 55.9-fold higher in samples incubated with the CAPRIN2 antibody in comparison to the non-specific IgG (Fig. 9a). Moreover, *Oxt* mRNA levels in the SON and PVN of salt loaded rats were also 21.4- and 47.7-fold, respectively, higher in samples incubated with CAPRIN2 antibodies (Fig. 9a). This indicates that CAPRIN2 can bind the *Oxt* mRNA in the SON and PVN in euhydrated and salt-loaded conditions. To further assess the effect of salt loading in relation to the amount of CAPRIN2-bound *Oxt* transcripts, we compared CAPRIN2-bound fractions in salt-loaded rats in comparison to euhydrated animals. Similar results were observed for the SON and the PVN, where significant higher levels of CAPRIN2-bound *Oxt* mRNA were observed in the salt loaded samples (1.14 ± 0.32 in euhydrated rats vs 2.14 ± 0.22 in salt-loaded rats in the SON and 1.01 ± 0.07 in euhydrated rats vs 3 ± 0.75 in salt-loaded animals in the PVN; Fig. 9b). Altogether the data indicates that CAPRIN2 binds *Oxt* mRNA in the SON and the PVN and that binding increases in response to salt loading.

Then, to assess if CAPRIN2 binding to *Oxt* mRNA increases its poly(A) tail length, we quantified transcript sizes by Northern blot in salt-loaded control (scrambled shRNA-injected) and CAPRIN2KD (Caprin2 shRNA-injected) rats. Salt-loading increased the *Oxt* mRNA poly(A) tail length in the SON (Fig. 9c) and the PVN (Fig. 9c'). Moreover, we also observed that knocking down CAPRIN2 prevents the salt-loading-induced increase in *Oxt* mRNA tail poly(A) both in the SON (Fig. 9d) and the PVN (Fig. 9d'). No changes were observed with the *Gapdh* mRNA (Figure 9e, e').

Discussion

In this study, we have characterised and compared the spatiotemporal dynamics of the expression of *Creb3l1* and *Caprin2* RNA and CREB3L1 and CAPRIN2 protein levels in euhydrated, dehydrated and rehydrated conditions. We have previously characterised these genes as being regulators of the expression of the antidiuretic hormone AVP, particularly in response to dehydration. By providing a detailed depiction of the expression of *Creb3l1* and *Caprin2* we have unravelled novel mechanisms that operate in OXT neurones in regulating water balance.

We demonstrate by RNA *in situ* hybridization that *Creb3l1* is expressed in AVP and OXT MCNs of the SON and the PVN, but to a greater extent in AVP neurones. In the SON, dehydration increases *Creb3l1* expression both in AVP and OXT MCNs, although its expression is significantly higher in AVP neurones. In contrast, dehydration increases *Creb3l1* expression exclusively in AVP neurones of the PVN. This is consistent with previous data where we demonstrated that CREB3L1 is activated predominantly in AVP neurones in response to dehydration [16], but it also indicates that CREB3L1 might play a role in OXT neurones. In contrast, the labelling of *Caprin2* mRNA revealed that *Caprin2* is equally present in both AVP and OXT neurones in euhydrated basal conditions and that, in response to hyperosmotic stress, its expression increases in both neuronal types to same extent. The increase in *Creb3l1* abundance in AVP and OXT MCNs in response to osmotic stimulation may be mediated by the orphan nuclear receptor Nr4a1. We previously identified that *Creb3l1* transcription can be regulated by Nr4a1 interactions with a NBRE site in the *Creb3l1* promoter [29] and Nr4a1 is increased in both cell-types by osmotic stimulation to support this concept [30]. Furthermore, dual overexpression of transcription factors *Atf4* and *Fosl1* in HMLE cells has been reported to promote *Creb3l1* expression [31]. The expression of both *Atf4* and *Fosl1* increase in the SON following osmotic

stress [32, 12], thus proposing an additional mechanism for the regulation of *Creb3l1* expression. To our knowledge, the mechanisms that regulate *Caprin2* transcription remain unknown.

It is widely accepted that RNA levels and protein abundance do not necessarily correlate [18, 26, 27]. We simultaneously labelled *Creb3l1* and *Caprin2* RNA and CREB3L1 and CAPRIN2 protein and found a strong relationship between transcript and protein abundance in all experimental conditions. This indicates that *Creb3l1* and *Caprin2* mRNA abundance reflects protein levels changes in MCNs of the hypothalamus and, hence, these events have biological significance. Whilst the functions of CREB3L1 and CAPRIN2 have already been investigated in the AVP-ergic system, their OXT-ergic system functions have been ignored despite OXT MCNs being robustly activated by osmotic stimuli [33], which includes increased expression of heteronuclear [9] and mature *Oxt* RNA [11, 12], and elevated OXT release to promote natriuresis [3, 9]. In the present data, we found that the CREB3L1 increases in OXT neurones in response to dehydration and our findings *in vitro* imply that CREB3L1 may regulate *Oxt* transcription. The absence of canonical CREB3L1 binding motifs in the *Oxt* promoter raises three possibilities in respect to the increased luciferase activity by CREB3L1 *in vitro*: 1) that CREB3L1 binds to the *Oxt* promoter directly in a non-canonical site, 2) that CREB3L1 binds to the *Oxt* promoter as part of a complex or that 3) CREB3L1 regulates *Oxt* transcription indirectly by regulating other transcription factors. Thus, we propose that osmotically stimulated increases in OXT neurone CREB3L1 expression are important for increased OXT synthesis. We similarly identify that CAPRIN2 expression also increases in OXT neurones and demonstrate that CAPRIN2 binds *Oxt* RNA and mediates the increase in *Oxt* mRNA poly(A) tail length that accompanies osmotic stimulation. Therefore, we propose that CAPRIN2 facilitates post-transcriptional modifications that increase *Oxt* transcript stability. In addition, we have identified *Oxt* mRNA as an additional RNA binding partner of CAPRIN2 as, since its discovery as an RNA binding protein in 2010 [19], to our knowledge, the only RNA binding partner identified so far has been *Avp* mRNA [21]. All the above illustrates that there are common mechanisms in AVP and OXT neurones, involving CREB3L1 and CAPRIN2, that operate in response to osmotic stress to regulate AVP and OXT synthesis. It is known that *Avp* and *Oxt* RNA increase in response to osmotic stimuli such as dehydration and salt loading [34, 9]. Interestingly, there is a more robust increase in *Oxt* transcription in response to salt loading in comparison to dehydration, perhaps indicating the important role of OXT in natriuresis in response to high salt intake. The question now is whether these mechanisms also operate in response to stimuli that solely or mainly activate OXT neurones, such as lactation. Further studies addressing this issue will shed light on the mechanisms that regulate OXT synthesis.

In relation to the striking *Caprin2* mRNA labelling in the nucleus following osmotic stimulation, we have labelled *Caprin2* mRNA in combination with different mRNA and proteins specific for distinct nuclear bodies, in order to gain insight into a possible role for *Caprin2* mRNA in the nucleus. We found that *Caprin2* mRNA did not localise to any nuclear regions explored in this study, which included the nucleolus, cajal bodies, nuclear speckles and nuclear paraspeckles. Instead, it appears that *Caprin2* is diffuse throughout the whole nucleus. The nuclear localisation of *Caprin2* mRNA raises interesting questions regarding its function. RNA molecules have been previously identified in the nucleus; however, these mainly include long non-coding RNAs [35], hyper-edited mRNAs [36] or incompletely spliced mRNAs [37, 38], whilst nuclear retention of mature protein-coding mRNA has traditionally been considered uncommon in mammals. However, there is growing evidence suggesting that some protein-coding mRNAs are retained in the nucleus, thus regulating gene expression [39, 40]. It has been suggested that the cell nucleus might be retaining RNA molecules that are not immediately required for translation, but that are rapidly needed in the cytoplasm to produce proteins in response to physiologic stress [39]. It has also been suggested that the retention

of mRNA in the nucleus might serve to buffer transcript levels in the cytoplasm from noise generated from transcriptional bursts [40]. Interestingly, some of these nuclear-retained RNAs have been observed to be preferentially localised either in paraspeckles [39], speckles [40], or, consistent with the present study, diffusely distributed throughout the nuclei [39]. In view of the response of *Caprin2* mRNA to dehydration, it is possible that *Caprin2* mRNA might be being harboured in the nucleus and only delivered to the cytosol when needed, but the mechanisms leading to *Caprin2* mRNA nuclear localisation, and its possible functions need to be further investigated. This contrasts with the locations of the *Avp* and *Oxt* RNAs that are mainly found in the cytoplasm compartment, both in euhydrated and dehydrated conditions, despite the vast quantities produced in response to osmotic stress.

In summary, we show that dehydration increases the mRNA and protein expression of *Creb3l1/*CREB3L1 and *Caprin2*/CAPRIN2 in AVP and OXT neurones. While it was already known that CREB3L1 and CAPRIN2 regulate *Avp* transcription and mRNA poly(A) tail length, respectively, we now provide compelling evidence of twinned roles in the regulation of OXT neurones. Interestingly, we found nuclear aggregations of *Caprin2* mRNA, enhanced by dehydration, that distribute diffusively around the nucleus, possibly to regulate *Caprin2* mRNA availability in the cytoplasm and to protect from the transcriptional burst in response to dehydration. We show how studying the expression dynamics of genes in MCNs can bring new perspectives to study their roles in water homeostasis, which can ultimately have an impact on hydration and well-being.

Statements

Acknowledgement

The authors gratefully acknowledge the Wolfson Bioimaging Facility for their support and assistance in this work.

Statement of Ethics

All experimental procedures involving animals were performed in strict accordance with the provision of the UK Animals (Scientific Procedures) Act (1986). The study was carried out under a Home Office UK licence (PPL 30/3278) and all the protocols were approved by the University of Bristol Animal Welfare and Ethical Review Board.

Conflict of Interest Statement

The authors have no conflicts of interest to declare.

Funding Sources

This research was supported by the BBSRC (Grant Number BB/R016879/1) to DM, SB-L, MPG and the Leverhulme Trust (Grant Number RPG-2017-287) to DM, MPG.

Author Contributions

SB-L: Conceptualisation; Formal analysis; Investigation; Methodology; Project administration; Writing – original draft; Writing – review & editing. **AK**: Formal analysis; Investigation; Writing – review & editing. **SJC**: Formal analysis; Software development; Writing – review & editing. **MG**: Formal analysis; Investigation; Writing – review & editing. **MS**: Formal analysis; Writing – review & editing. **DM**: Conceptualisation; Funding acquisition; Project administration; Supervision; Writing – review & editing. **MPG**: Conceptualisation; Formal analysis; Investigation; Methodology; Project administration; Supervision; Writing – review & editing

Data Availability Statement

All data generated and analysed during this study are included in this article. Further enquiries can be directed to the corresponding author.

References

1. Barez-Lopez S, Scanlon L, Murphy D, Greenwood MP. Imaging the hypothalamo-neurohypophysial system. Neuroendocrinology. 2021 Aug 26.
2. Burbach JP, Luckman SM, Murphy D, Gainer H. Gene regulation in the magnocellular hypothalamo-neurohypophysial system. Physiol Rev. 2001 Jul;81(3):1197-267.
3. Balment RJ, Brimble MJ, Forsling ML. Release of oxytocin induced by salt loading and its influence on renal excretion in the male rat. J Physiol. 1980 Nov;308:439-49.
4. Huang W, Lee SL, Sjoquist M. Natriuretic role of endogenous oxytocin in male rats infused with hypertonic NaCl. Am J Physiol. 1995 Mar;268(3 Pt 2):R634-40.
5. Huang W, Lee SL, Arnason SS, Sjoquist M. Dehydration natriuresis in male rats is mediated by oxytocin. Am J Physiol. 1996 Feb;270(2 Pt 2):R427-33.
6. Verbalis JG, Mangione MP, Stricker EM. Oxytocin produces natriuresis in rats at physiological plasma concentrations. Endocrinology. 1991 Mar;128(3):1317-22.
7. Soares TJ, Coimbra TM, Martins AR, Pereira AG, Carnio EC, Branco LG, et al. Atrial natriuretic peptide and oxytocin induce natriuresis by release of cGMP. Proc Natl Acad Sci U S A. 1999 Jan 5;96(1):278-83.
8. Kondo N, Arima H, Banno R, Kuwahara S, Sato I, Oiso Y. Osmoregulation of vasopressin release and gene transcription under acute and chronic hypovolemia in rats. Am J Physiol Endocrinol Metab. 2004 Mar;286(3):E337-46.
9. Greenwood MP, Mecawi AS, Hoe SZ, Mustafa MR, Johnson KR, Al-Mahmoud GA, et al. A comparison of physiological and transcriptome responses to water deprivation and salt loading in the rat supraoptic nucleus. Am J Physiol Regul Integr Comp Physiol. 2015 Apr 1;308(7):R559-68.
10. Sherman TG, Civelli O, Douglass J, Herbert E, Watson SJ. Coordinate expression of hypothalamic pro-dynorphin and pro-vasopressin mRNAs with osmotic stimulation. Neuroendocrinology. 1986;44(2):222-8.
11. Carter DA, Murphy D. Independent regulation of neuropeptide mRNA level and poly(A) tail length. J Biol Chem. 1989 Apr 25;264(12):6601-3.
12. Pauza AG, Mecawi AS, Paterson A, Hindmarch CCT, Greenwood M, Murphy D, et al. Osmoregulation of the transcriptome of the hypothalamic supraoptic nucleus: A resource for the community. J Neuroendocrinol. 2021 Jun 22;33(8):e13007.
13. Carrazana EJ, Pasieka KB, Majzoub JA. The vasopressin mRNA poly(A) tract is unusually long and increases during stimulation of vasopressin gene expression in vivo. Mol Cell Biol. 1988 Jun;8(6):2267-74.
14. Murphy D, Carter D. Vasopressin gene expression in the rodent hypothalamus: transcriptional and posttranscriptional responses to physiological stimulation. Mol Endocrinol. 1990 Jul;4(7):1051-9.
15. Carter DA, Murphy D. Rapid changes in poly (A) tail length of vasopressin and oxytocin mRNAs form a common early component of neurohypophyseal peptide gene activation following physiological stimulation. Neuroendocrinology. 1991 Jan;53(1):1-6.
16. Greenwood M, Bordieri L, Greenwood MP, Rosso Melo M, Colombari DS, Colombari E, et al. Transcription factor CREB3L1 regulates vasopressin gene expression in the rat hypothalamus. J Neurosci. 2014 Mar 12;34(11):3810-20.
17. Stewart L, Hindmarch CC, Qiu J, Tung YC, Yeo GS, Murphy D. Hypothalamic transcriptome plasticity in two rodent species reveals divergent differential gene expression but conserved pathways. J Neuroendocrinol. 2011 Feb;23(2):177-85.
18. Greenwood M, Greenwood MP, Mecawi AS, Loh SY, Rodrigues JA, Paton JF, et al. Transcription factor CREB3L1 mediates cAMP and glucocorticoid regulation of arginine vasopressin gene transcription in the rat hypothalamus. Mol Brain. 2015 Oct 26;8(1):68.

19. Shiina N, Tokunaga M. RNA granule protein 140 (RNG140), a paralog of RNG105 localized to distinct RNA granules in neuronal dendrites in the adult vertebrate brain. J Biol Chem. 2010 Jul 30;285(31):24260-9.
20. Loh SY, Jahans-Price T, Greenwood MP, Greenwood M, Hoe SZ, Konopacka A, et al. Unsupervised Network Analysis of the Plastic Supraoptic Nucleus Transcriptome Predicts Caprin2 Regulatory Interactions. eNeuro. 2017 Nov-Dec;4(6).
21. Konopacka A, Greenwood M, Loh SY, Paton J, Murphy D. RNA binding protein Caprin-2 is a pivotal regulator of the central osmotic defense response. Elife. 2015 Nov 12;4.
22. de Sousa Abreu R, Penalva LO, Marcotte EM, Vogel C. Global signatures of protein and mRNA expression levels. Mol Biosyst. 2009 Dec;5(12):1512-26.
23. Schwanhausser B, Busse D, Li N, Dittmar G, Schuchhardt J, Wolf J, et al. Global quantification of mammalian gene expression control. Nature. 2011 May 19;473(7347):337-42.
24. Pederson T. The nucleolus. Cold Spring Harb Perspect Biol. 2011 Mar 1;3(3).
25. Sawyer IA, Sturgill D, Sung MH, Hager GL, Dundr M. Cajal body function in genome organization and transcriptome diversity. Bioessays. 2016 Dec;38(12):1197-208.
26. Fox AH, Lamond AI. Paraspeckles. Cold Spring Harb Perspect Biol. 2010 Jul;2(7):a000687.
27. Lamond AI, Spector DL. Nuclear speckles: a model for nuclear organelles. Nat Rev Mol Cell Biol. 2003 Aug;4(8):605-12.
28. Spector DL, Lamond AI. Nuclear speckles. Cold Spring Harb Perspect Biol. 2011 Feb 1;3(2).
29. Greenwood MP, Greenwood M, Gillard BT, Chitra Devi R, Murphy D. Regulation of cAMP Responsive Element Binding Protein 3-Like 1 (Creb3l1) Expression by Orphan Nuclear Receptor Nr4a1. Front Mol Neurosci. 2017;10:413.
30. Chan RK, Brown ER, Ericsson A, Kovacs KJ, Sawchenko PE. A comparison of two immediate-early genes, c-fos and NGFI-B, as markers for functional activation in stress-related neuroendocrine circuitry. J Neurosci. 1993 Dec;13(12):5126-38.
31. Feng YX, Jin DX, Sokol ES, Reinhardt F, Miller DH, Gupta PB. Cancer-specific PERK signaling drives invasion and metastasis through CREB3L1. Nat Commun. 2017 Oct 20;8(1):1079.
32. Greenwood M, Greenwood MP, Paton JF, Murphy D. Transcription Factor CREB3L1 Regulates Endoplasmic Reticulum Stress Response Genes in the Osmotically Challenged Rat Hypothalamus. PLoS One. 2015;10(4):e0124956.
33. Giovannelli L, Shiromani PJ, Jirikowski GF, Bloom FE. Oxytocin neurons in the rat hypothalamus exhibit c-fos immunoreactivity upon osmotic stress. Brain Res. 1990 Oct 29;531(1-2):299-303.
34. Greenwood MP, Greenwood M, Paton JF, Murphy D. Salt appetite is reduced by a single experience of drinking hypertonic saline in the adult rat. PLoS One. 2014;9(8):e104802.
35. West JA, Davis CP, Sunwoo H, Simon MD, Sadreyev RI, Wang PI, et al. The long noncoding RNAs NEAT1 and MALAT1 bind active chromatin sites. Mol Cell. 2014 Sep 4;55(5):791-802.
36. Chen LL, Carmichael GG. Altered nuclear retention of mRNAs containing inverted repeats in human embryonic stem cells: functional role of a nuclear noncoding RNA. Mol Cell. 2009 Aug 28;35(4):467-78.
37. Shalgi R, Hurt JA, Lindquist S, Burge CB. Widespread inhibition of posttranscriptional splicing shapes the cellular transcriptome following heat shock. Cell Rep. 2014 Jun 12;7(5):1362-70.
38. Boutz PL, Bhutkar A, Sharp PA. Detained introns are a novel, widespread class of post-transcriptionally spliced introns. Genes Dev. 2015 Jan 1;29(1):63-80.
39. Prasanth KV, Prasanth SG, Xuan Z, Hearn S, Freier SM, Bennett CF, et al. Regulating gene expression through RNA nuclear retention. Cell. 2005 Oct 21;123(2):249-63.
40. Bahar Halpern K, Caspi I, Lemze D, Levy M, Landen S, Elinav E, et al. Nuclear Retention of mRNA in Mammalian Tissues. Cell Rep. 2015 Dec 29;13(12):2653-62.

Figure Legends

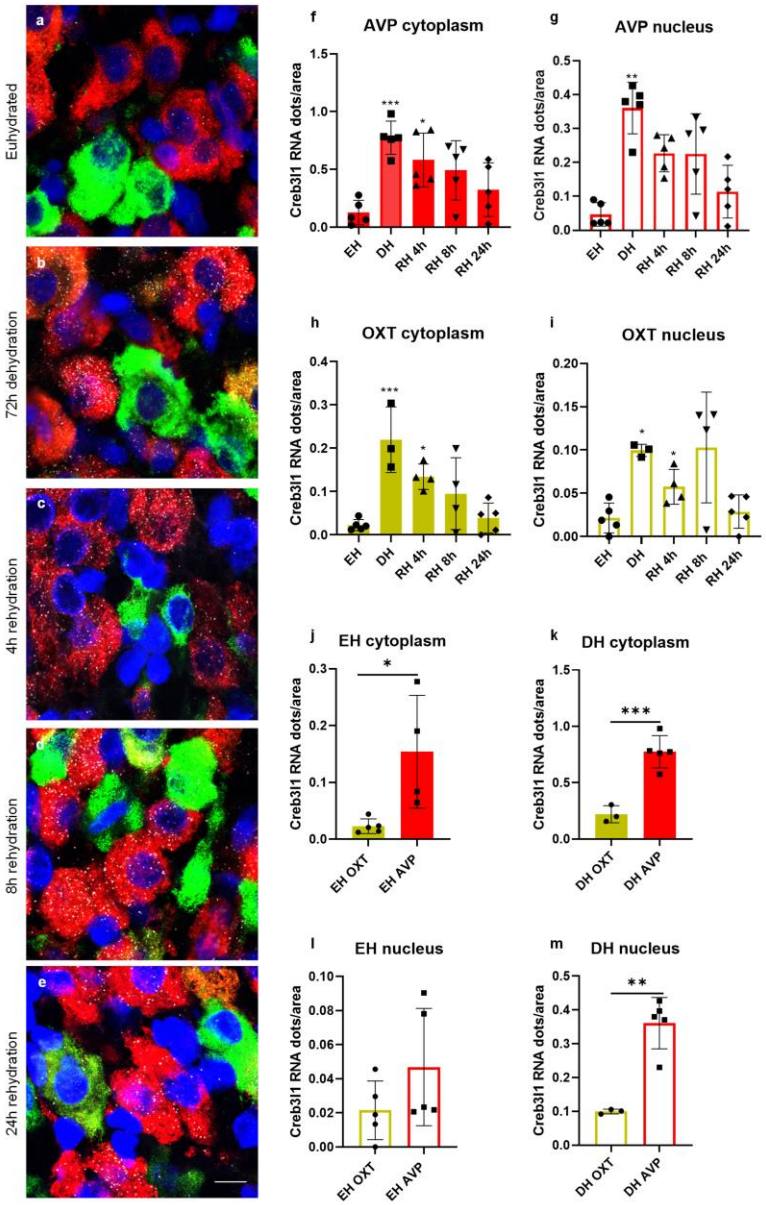

Fig. 1. *Creb3l1* mRNA expression in the SON labelled by RNAscope *in situ* hybridisation in euhydrated (EH; nAVP = 5, nOXT = 5) conditions (**a**), after 72 hours of dehydration (DH; nAVP = 5, nOXT = 3, **b**), after 72 hours dehydration followed by 4 hours rehydration (RH 4h; nAVP = 5, nOXT = 4, **c**), after 72 hours dehydration followed by 8 hours rehydration (RH 8h; nAVP = 5, nOXT = 4, **d**) and after 72 hours dehydration followed by 24 hours rehydration (RH 24 h; nAVP = 5, nOXT = 5, **e**). DAPI: blue, *Avp*: red, *Oxt*: green, *Creb3l1*: white. Graphs showing gene expression as a function of Creb3l1 mRNA dots/cytoplasm AVP neurones (**f**), Creb3l1 mRNA dots/nuclei AVP neurones (**g**), Creb3l1 mRNA dots/cytoplasm OXT neurones (**h**), Creb3l1 mRNA dots/nuclei OXT neurones (**i**), Creb3l1 mRNA dots/cytoplasm of AVP vs OXT neurones in EH conditions (**j**), Creb3l1 mRNA dots/cytoplasm of AVP vs OXT neurones in DH conditions (**k**), Creb3l1 mRNA dots/nuclei of AVP vs OXT neurones in EH conditions (**l**), and Creb3l1 mRNA dots/nuclei of AVP vs OXT neurones in DH conditions (**m**). Data are expressed as mean ± SD and *P < 0.05; **P < 0.01, and ***P < 0.001 indicate statistically significant differences with the EH group. Scale bar represents 10 µm.

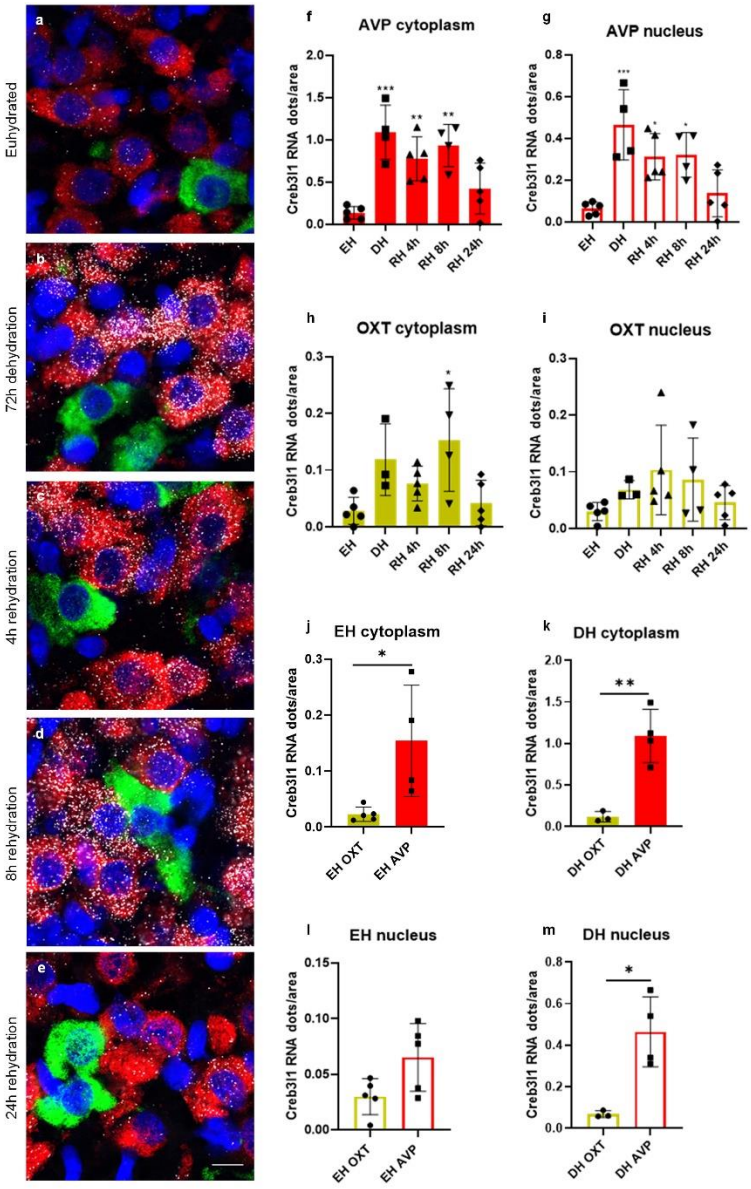

Fig. 2. *Creb3l1* mRNA expression in the PVN labelled by RNAscope *in situ* hybridisation in euhydrated (EH; nAVP = 5, nOXT = 5) conditions (**a**), after 72 hours of dehydration (DH; nAVP = 4, nOXT = 3, **b**), after 72 hours dehydration followed by 4 hours rehydration (RH 4h; nAVP = 5, nOXT = 5, **c**), after 72 hours dehydration followed by 8 hours rehydration (RH 8h; nAVP = 4, nOXT = 4, **d**) and after 72 hours dehydration followed by 24 hours rehydration (RH 24 h; nAVP = 5, nOXT = 5, **e**). DAPI: blue, *Avp*: red, *Oxt*: green, *Creb3l1*: white. Graphs showing gene expression as a function of Creb3l1 mRNA dots/cytoplasm AVP neurones (**f**), Creb3l1 mRNA dots/nuclei AVP neurones (**g**), Creb3l1 mRNA dots/cytoplasm OXT neurones (**h**), Creb3l1 mRNA dots/nuclei OXT neurones (**i**), Creb3l1 mRNA dots/cytoplasm of AVP vs OXT neurones in EH conditions (**j**), Creb3l1 mRNA dots/cytoplasm of AVP vs OXT neurones in DH conditions (**k**), Creb3l1 mRNA dots/nuclei of AVP vs OXT neurones in EH conditions (**l**), and Creb3l1 mRNA dots/nuclei of AVP vs OXT neurones in DH conditions (**m**). Data are expressed as mean ± SD and *P < 0.05; **P < 0.01, and ***P < 0.001 indicate statistically significant differences with the EH group. Scale bar represents 10 µm.

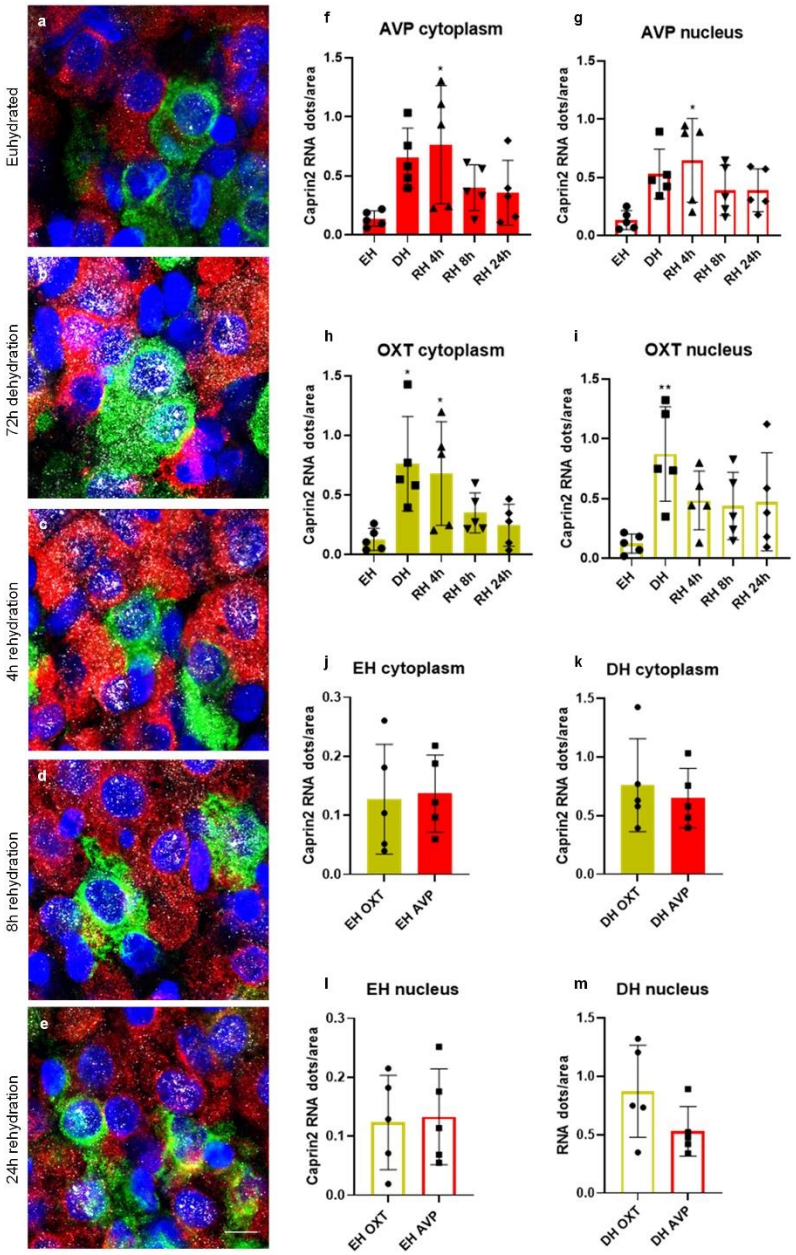

Fig. 3. *Caprin2* mRNA expression in the SON labelled by RNAscope *in situ* hybridisation in euhydrated (EH; nAVP = 5, nOXT = 5) conditions (**a**), after 72 hours of dehydration (DH; nAVP = 5, nOXT = 5, **b**), after 72 hours dehydration followed by 4 hours rehydration (RH 4h; nAVP = 5, nOXT = 5, **c**), after 72 hours dehydration followed by 8 hours rehydration (RH 8h; nAVP = 5, nOXT = 5, **d**) and after 72 hours dehydration followed by 24 hours rehydration (RH 24 h; nAVP = 5, nOXT = 5, **e**). DAPI: blue, *Avp*: red, *Oxt*: green, *Caprin2*: white. Graphs showing gene expression as a function of Caprin2 mRNA dots/cytoplasm AVP neurones (**f**), Caprin2 mRNA dots/nuclei AVP neurones (**g**), Caprin2 mRNA dots/cytoplasm OXT neurones (**h**), Caprin2 mRNA dots/nuclei OXT neurones (**i**), Caprin2 mRNA dots/cytoplasm of AVP vs OXT neurones in EH conditions (**j**), Caprin2 mRNA dots/cytoplasm of AVP vs OXT neurones in DH conditions (**k**), Caprin2 mRNA dots/nuclei of AVP vs OXT neurones in EH conditions (**l**), and Caprin2 mRNA dots/nuclei of AVP vs OXT neurones in DH conditions (**m**). Data are expressed as mean ± SD and *P < 0.05; **P < 0.01, and ***P < 0.001 indicate statistically significant differences with the EH group. Scale bar represents 10 µm.

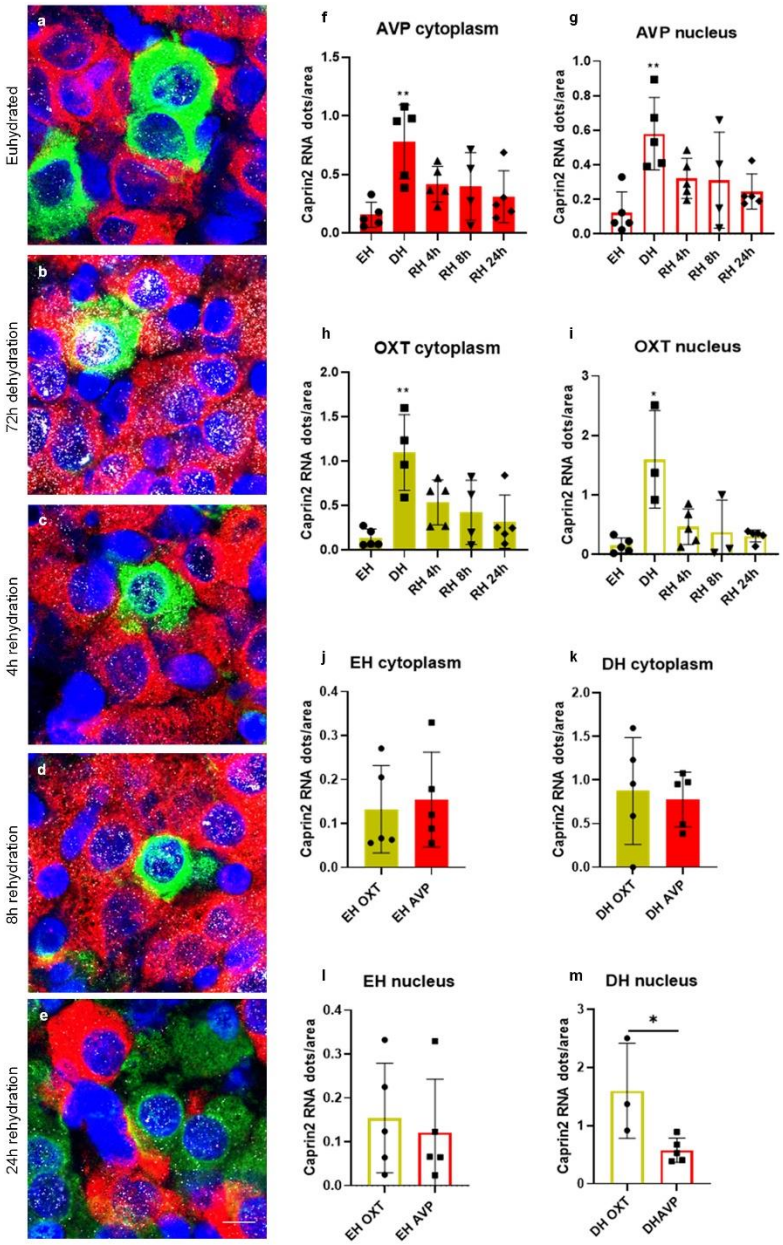

Fig. 4. *Caprin2* mRNA expression in the PVN labelled by RNAscope *in situ* hybridisation in euhydrated (EH; nAVP = 5, nOXT = 5) conditions (**a**), after 72 hours of dehydration (DH; nAVP = 5, nOXT = 4, **b**), after 72 hours dehydration followed by 4 hours rehydration (RH 4h; nAVP = 5, nOXT = 5, **c**), after 72 hours dehydration followed by 8 hours rehydration (RH 8h; nAVP = 4, nOXT = 4, **d**) and after 72 hours dehydration followed by 24 hours rehydration (RH 24 h; nAVP = 5, nOXT = 5, **e**). DAPI: blue, *Avp*: red, *Oxt*: green, *Caprin2*: white. Graphs showing gene expression as a function of Caprin2 mRNA dots/cytoplasm AVP neurones (**f**), Caprin2 mRNA dots/nuclei AVP neurones (**g**), Caprin2 mRNA dots/cytoplasm OXT neurones (**h**), Caprin2 mRNA dots/nuclei OXT neurones (**i**), Caprin2 mRNA dots/cytoplasm of AVP vs OXT neurones in EH conditions (**j**), Caprin2 mRNA dots/cytoplasm of AVP vs OXT neurones in DH conditions (**k**), Caprin2 mRNA dots/nuclei of AVP vs OXT neurones in EH conditions (**l**), and Caprin2 mRNA dots/nuclei of AVP vs OXT neurones in DH conditions (**m**). Data are expressed as mean ± SD and *P < 0.05; **P < 0.01, and ***P < 0.001 indicate statistically significant differences with the EH group. Scale bar represents 10 µm.

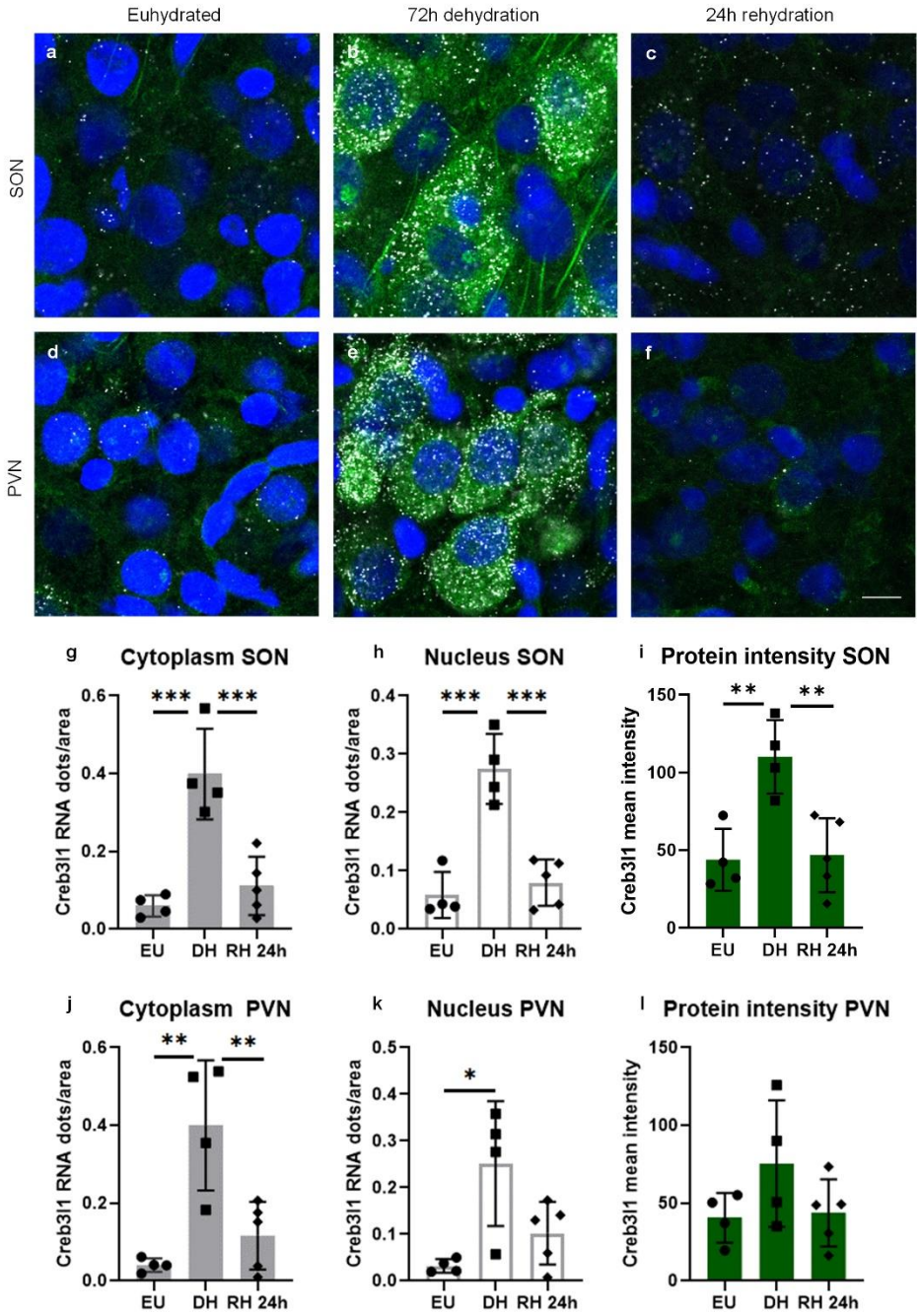

Fig. 5. *Creb3l1* mRNA expression labelled by RNAscope *in situ* hybridisation in combination with CREB3L1 protein labelling by immunohistochemistry in euhydrated (EH; nSON = 4, nPVN = 4) conditions (**a**), after 72 hours of dehydration (DH; nSON = 4, nPVN = 4, **b**), and after 72 hours dehydration followed by 24 hours rehydration (RH 24 h; nSON = 5, nPVN = 5, **c**) in the SON. Creb3l1 mRNA and protein labelling in EH (**d**), DH (**e**), and RH 24 hours (**f**) conditions in the PVN. DAPI: blue, *Creb3l1* mRNA: white, CREB3L1 protein: green. Graphs showing gene expression as a function of *Creb3l1* mRNA dots/cytoplasm (**g**), *Creb3l1* mRNA dots/nuclei (**h**), and CREB3L1 protein intensity values (**i**) in the SON. Graphs showing gene expression as a function of *Creb3l1* mRNA dots/cytoplasm (**j**), *Creb3l1* mRNA dots/nuclei (**k**), and CREB3L1 protein intensity values (**l**) in the PVN. Data are expressed as mean ± SD and *P < 0.05; **P < 0.01, and ***P < 0.001. Scale bar represents 10 µm.

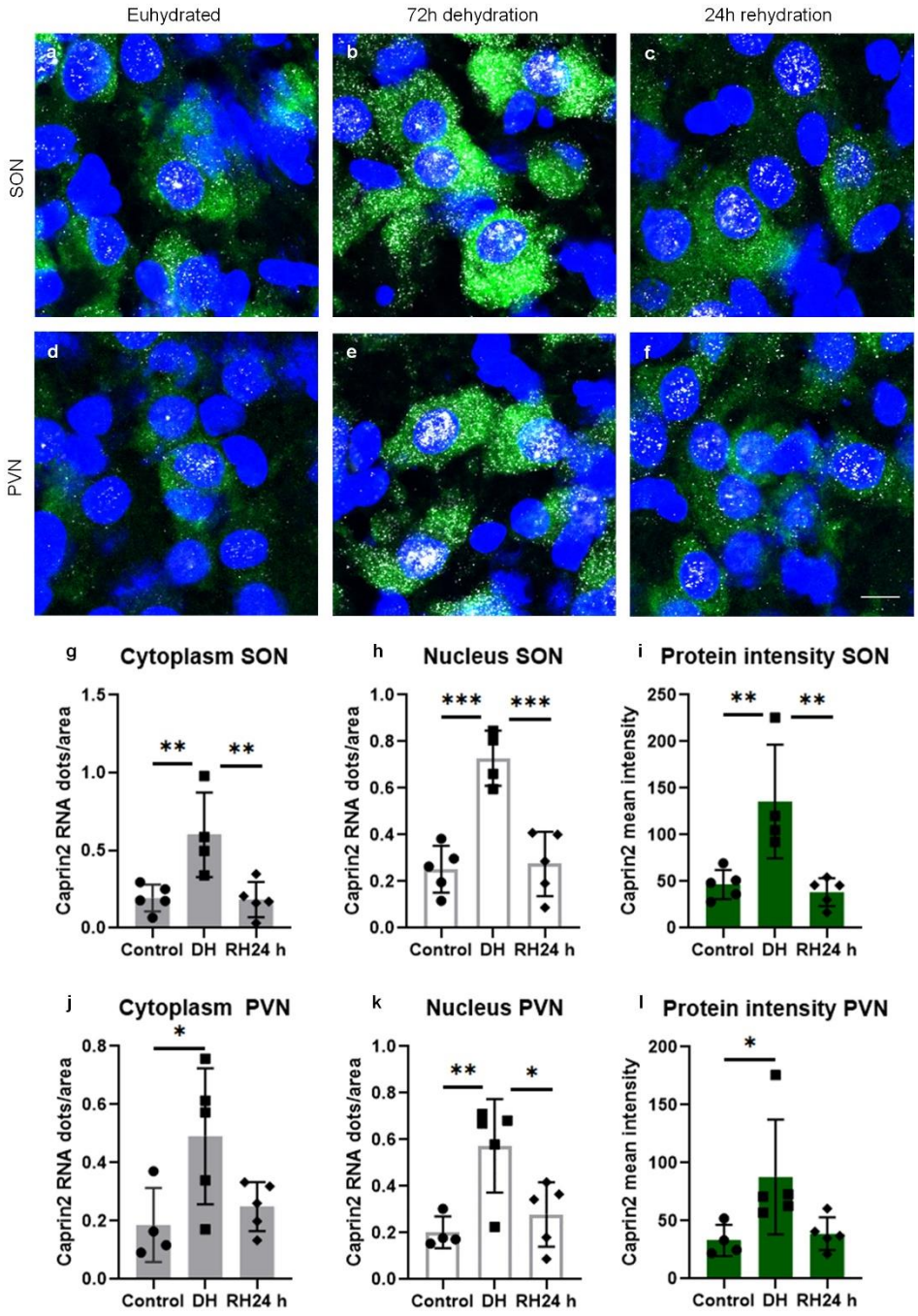

Fig. 6. *Caprin2* mRNA expression labelled by RNAscope *in situ* hybridisation in combination with CAPRIN2 protein labelling by immunohistochemistry in euhydrated (EH; nSON = 5, nPVN = 4) conditions (**a**), after 72 hours of dehydration (DH; nSON = 4, nPVN = 5, **b**), and after 72 hours dehydration followed by 24 hours rehydration (RH 24 h; nSON = 5, nPVN = 5, **c**) in the SON. Caprin2 mRNA and protein labelling in EH (**d**), DH (**e**), and RH 24 hours (**f**) conditions in the PVN. DAPI: blue, *Caprin2* mRNA: white, CAPRIN2 protein: green. Graphs showing gene expression as a function of *Caprin2* mRNA dots/cytoplasm (**g**), *Caprin2* mRNA dots/nuclei (**h**), and CAPRIN2 protein intensity values (**i**) in the SON. Graphs showing gene expression as a function of *Caprin2* mRNA dots/cytoplasm (**j**), *Caprin2* mRNA dots/nuclei (**k**), and CAPRIN2 protein intensity values (**l**) in the PVN. Data are expressed as mean ± SD and *P < 0.05; **P < 0.01, and ***P < 0.001. Scale bar represents 10 µm.

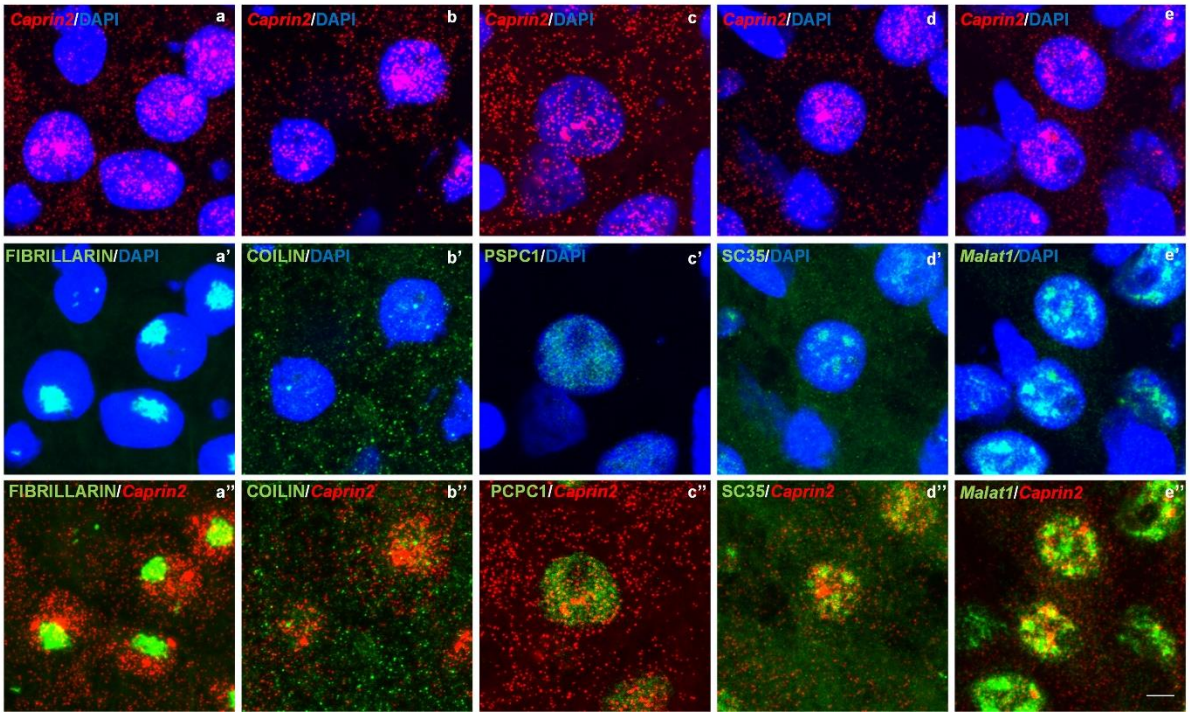

Fig. 7. *Caprin2* mRNA labelled by RNAscope *in situ* hybridisation (red; **a**, **b**, **c**, **d**, **e**) in combination with immunolabelling of the nuclear bodies markers NUCLEOLIN (green: **a'**), COILIN (green, **b'**), PSPC1 (green, **c'**), SC35 (green, **d'**) and RNAscope *in situ* hybridisation labelling of *Malat1* (green, **e'**) with nuclei counterstained with DAPI (blue), in the SON after 72 hours of dehydration (n = 4). Merge of *Caprin2* mRNA labelling with NUCLEOLIN (**a''**), COILIN (**b''**), PSPC1 (**c''**), SC35 (**d''**) and *Malat1* (**e''**) with DAPI removed to allow for better visualisation of localization of *Caprin2* mRNA and nuclear bodies markers. Scale bar represents 5 µm.

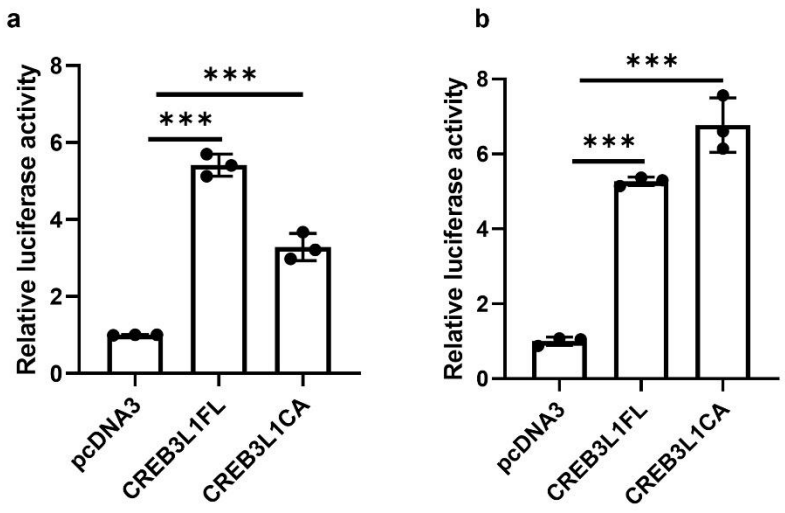

c

-197 GAGCTCC**AGGTCA**TTAGCTGAGGCGG**TGACCTTGACC**CCAGCCCAGACCC -148

-147 TGCAAATGAAGGGCCTGCTTCTAAACAGTGTGGAACAGTT**TGACC**CAAGA -98

-97 GACCTGCTG**TGACC**AGTCATGCAGTCACCCTCTTTAGACTGGGCCCCACCA -48

-47 TGGCAGTGGCCAGGCATAAAAAGGTCGGTCTGGGCTGGAGAAACCA -1

d

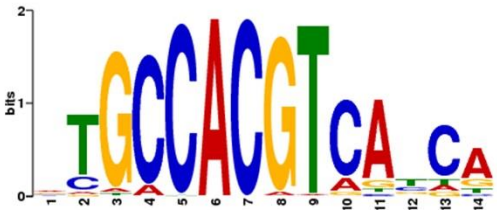

Fig. 8. CREB3L1 can regulate *Oxt* transcription. Luciferase assays were performed in HEK293T cells transfected with plasmid containing (**a**) 822 bp rat *Oxt* promoter together with plasmids expressing full-length CREB3L1 (CREB3L1FL) or the constitutively active form of CREB3L1 (CREB3L1CA), or (**b**) 197 bp rat *Oxt* promoter together with plasmids expressing CREB3L1FL or CREB3L1CA. (c) The main known regulatory motifs contained in the 197bp promoter region flanking the OXT gene. The positions of previously identified oestrogen response element motifs are indicated by bold text. The TATA box equivalent is boxed. (d) No canonical CREB3L1 binding motifs are present in this region of the OXT promoter. Data are expressed as mean ± SD (n = 3) and ***P < 0.001.

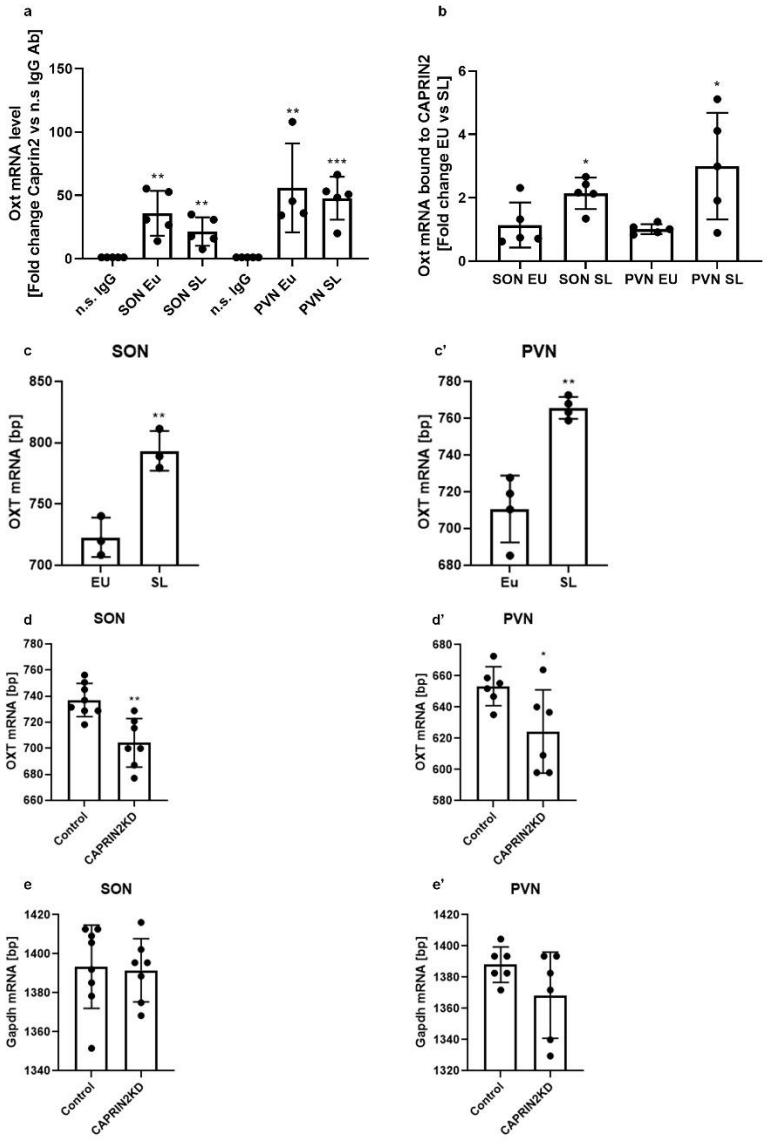

Fig. 9. (**a**) Binding *Oxt* mRNA by CAPRIN2 in the SON and PVN of euhydrated (EU; nSON = 5, nPVN = 4) and salt-loaded (SL; nSON = 5, nPVN = 5) rats determined by RNA immunoprecipitation assay. *Oxt* mRNA levels bound to CAPRIN2, expressed as a ratio of mRNA detected in CAPRIN2 immunoprecipitate vs. non-specific IgG (n.s.) immunoprecipitate. (**b**) Effects of salt-loading on the levels of *Oxt* mRNA bound to CAPRIN2 in the SON (nEU = 5, nSL = 5) and the PVN (nEU = 5, nSL = 5). (**c**) Effects of salt-loading on the length of poly(A) tails in *Oxt* mRNAs determined by Northern blot analysis in the SON of naïve rats (nEU = 3, nSL = 3) and (**c'**) Effects of salt-loading on the length of poly(A) tails in *Oxt* mRNAs determined by Northern blot analysis in the PVN of naïve rats (nEU = 4, nSL = 4). (**d**) Effects of salt-loading on the length of poly(A) tails in *Oxt* mRNAs determined by Northern blot analysis in the SON of control (scrambled shRNA-injected; n = 8) and CAPRIN2KD (Caprin2 shRNA-injected; 7) rats. (**d'**) Effects of salt-loading on the length of poly(A) tails in *Oxt* mRNAs determined by Northern blot analysis in the PVN of control (n = 6) and CAPRIN2KD (n = 6) rats. (**e**) Northern blot analysis in the SON of control (n = 8) and CAPRIN2KD (n = 7) rats revealed no changes on the length of poly(A) tails in *Gapdh* mRNAs. (**e'**) Northern blot analysis in the PVN of control (n = 6) and CAPRIN2KD (n = 6) rats revealed no changes on the length of poly(A) tails in *Gapdh* mRNAs. Data are expressed as mean ± SD and **P < 0.01, and ***P < 0.001.